Osteoarthritis and Cartilage Open 6 (2024) 100450

Contents lists available at ScienceDirect

Osteoarthritis and Cartilage Open

journal homepage: www.elsevier.com/journals/osteoarthritis-and-cartilage-open/2665-9131

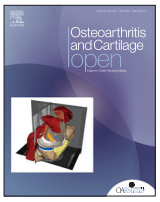

Effects of self-assembled type II collagen fibrils on the morphology and growth of pre-chondrogenic ATDC5 cells

Linyan Shi [a,*], Kazuhiro Ura [b], Yasuaki Takagi [b]

[a] Graduate School of Fisheries Sciences, Hokkaido University, 3-1-1 Minato-Cho, Hakodate, Hokkaido, 041-8611, Japan
[b] Faculty of Fisheries Sciences, Hokkaido University, 3-1-1 Minato-cho, Hakodate, Hokkaido, 041-8611, Japan

ARTICLE INFO

Handling Editor: Professor H Madry

Keywords:
Cartilage tissue engineering (CTE)
Scaffold
Marine type II collagen
Fibril biomaterial

ABSTRACT

Objective: Although type II collagen could have marked potential for developing cartilage tissue engineering (CTE) scaffolds, its erratic supply and viscous nature have limited these studies, and there are no studies on the use of marine-derived type II collagen fibrils for CTE scaffold materials. In this study, we aimed to generate a fibril-based, thin-layered scaffold from marine-derived type II collagen and investigate its chondrogenic potential.
Methods: Time-lapse observations revealed the cell adhesion process. The Cell Counting Kit-8 (CCK-8) assay, light microscopy, and scanning electron microscopy were performed to detect proliferation and filopodium morphology. Alcian blue staining was used to show the deposition of extracellular secretions, and qRT-PCR was performed to reveal the expression levels of chondrogenesis-related genes.
Results: The cell adhesion speed was similar in both fibril-coated and control molecule-coated groups, but the cellular morphology, proliferation, and chondrogenesis activity differed. On fibrils, more elongated finer filopodia showed inter-cell communications, whereas the slower proliferation suggested an altered cell cycle. Extracellular secretions occurred before day 14 and continued until day 28 on fibrils, and on fibrils, the expression of the chondrogenesis-related genes *Sox9* ($p < 0.001$), *Col10a1* ($p < 0.001$), *Acan* ($p < 0.001$), and *Col2a1* ($p = 0.0049$) was significantly upregulated on day 21.
Conclusion: Marine-derived type II collagen was, for the first time, fabricated into a fibril state. It showed rapid cellular affinity and induced chondrogenesis with extracellular secretions. We presented a new model for studying chondrogenesis *in vitro* and a potential alternative material for cell-laden CTE research.

1. Introduction

Mature articular cartilage (AC) tissues contain chondrocytes and an extracellular matrix (ECM) that functions as a scaffold for chondrocytes [1,2]. The major ECM components are type II collagen and proteoglycan (aggrecan), whose glycosaminoglycan chains are mainly composed of chondroitin sulfate [3,4]. Osteoarthritis (OA) is a chronic disease caused by joint wear or injury, and irreversible severe bone deterioration eventually leads to complete AC replacement surgery [5]. Traditionally, marrow stimulation, and allograft and autograft substitutions are clinically used for cartilage repair. However, these approaches have limitations such as quality deterioration, lack of integration, unideal cell viability, and additional defects [4,6,7]. Cartilage tissue engineering (CTE), in which scaffolds with or without cells replace deteriorated cartilage, is a promising approach for better clinical treatment. Currently, cell-laden scaffolds are widely studied in CTE, and several scaffold types have been reported [8–10].

Cell-laden scaffolds support cell proliferation and differentiation to achieve lesion repair after transplantation. Several studies have used type I collagen, the proportion of which is high in bones but low in cartilages, as a scaffold material [11,12]. However, clinical trials have also reported disadvantages of its use, such as incomplete cartilage repair [13]. In contrast, in a rabbit model with full-thickness articular cartilage defects, implants made of bovine type II collagen scaffolds reportedly repaired the cartilage better than those made of type I collagen [14]. Therefore, theoretically, using type II collagen to construct CTE scaffolds has become reasonable because type II collagen fibrils are a major component of cartilage ECM *in vivo* [15]. Type II collagen sources include domestic land animals (chickens, pigs, and cows) and sharks [16–18]. Owing to terrestrial animal-to-human disease transmission concerns, low-risk aquatic sources are considered suitable for biomaterial development [19]. However, this has endangered several shark species, and type II collagen yield from their cartilage is suboptimal [20]. Thus,

* Corresponding author.
E-mail addresses: shilinyan@eis.hokudai.ac.jp (L. Shi), kazu@fish.hokudai.ac.jp (K. Ura), takagi@fish.hokudai.ac.jp (Y. Takagi).

https://doi.org/10.1016/j.ocarto.2024.100450
Received 25 August 2023; Accepted 22 February 2024

alternative sources of type II collagen are needed for CTE scaffold development.

Type II collagen from the sturgeon notochord (NC), a by-product, was shown to be extractable with high efficiency [21]. Moreover, as this is an aquaculture species [22], a stable supply is guaranteed. Therefore, in this study, we aimed to materialize type II collagen from the NC, considering the requirements of CTE in scaffold development research, in search of a new CTE scaffold.

2. Materials and methods

2.1. Materials

The NC of Bester (*Huso huso* × *Acipenser ruthenus*), a hybrid species of sturgeon cultured in Bifuka Town, Hokkaido, Japan, was used in this study. Fresh NC samples were collected from the food workshop, subsequently vacuum-packed, and frozen; an uninterrupted cold chain was used to transport the material to the Faculty of Fisheries Sciences, Hokkaido University, Hokkaido, Japan. Type II collagen was purified from the NC, as described previously [21], without ethanol pretreatment. After lyophilization, the collagen was stored at −80 °C until use. ATDC5 cells were purchased from RIKEN Cell Bank (Tsukuba, Japan). The cell culture plates were obtained from Corning Inc. (Durham, NC, USA), and the penicillin-streptomycin (P/S) solution was obtained from Thermo Fisher Scientific (Waltham, MA, USA). Unless otherwise specified, all other reagents used in the cell culture experiments were purchased from Sigma-Aldrich Co., LLC. (St. Louis, MO, USA).

2.2. Preparation of coverslips coated with type II collagen fibrils

A new coating method to fabricate a thin layer of fibrils from type II collagen solution was developed and named the "flip-contact method". Lyophilized type II collagen powder was completely dissolved in an aqueous HCl solution (pH 3.0, 8 mg/mL) at 4 °C. Coverslips (φ = 13 mm; SARSTEDT Inc., Newton, NC, USA) were anchored to Petri dishes (φ = 9 cm, WISM; Mutoh Co., Tokyo, Japan) with minimal high-vacuum grease (Dow Corning Co., Midland, MI, USA). The collagen solution (35 μL) was pipetted onto each coverslip and smoothed on the surface using a cell scraper (1.8-cm blade; Corning, Tamaulipas, Mexico). The collagen-coated surface of the coverslip was then placed in contact with the surface of 30 mM Na-phosphate buffer (PB, pH 7.6) in a 24-well cell culture plate for at least 3 s. The coverslip was immersed in the PB with the coated surface facing upward. The plate was incubated at 12 °C for 48 h to form fibrils and for 48 h in 30 mM PB containing 1 mM genipin (FUJIFILM Wako Pure Chemical Corp., Osaka, Japan) to crosslink. After crosslinking, the coverslips were rinsed twice with Hank's balanced salt solution (HBSS) and immediately used in cell culture experiments. As controls, molecule-coated coverslips were prepared; 0.3 mg/mL type II collagen solution (35 μL) was smoothed on the coverslips, air-dried on a clean bench for 90 min at 21 °C, and crosslinked as described above. All procedures were performed under a clean bench, and the reagents, materials, and equipment used were sterilized for subsequent cell culture purposes.

2.3. Scanning electron microscopy (SEM) of fibrils

The coverslips were fixed with 2.5% (v/v) glutaraldehyde in PB (pH 7.6) for 2 h, dehydrated with increasing concentrations of ethanol, and finally immersed in t-butyl alcohol solution. After placing the samples overnight at −30 °C, they were freeze-dried (JFD-320; JEOL Ltd., Tokyo, Japan), coated with gold-platinum using a coater (JFC-1600; JEOL Ltd.), and observed under a scanning electron microscope (JSM6010LA; JEOL Ltd.). After capturing digital images, 300 fibrils were randomly selected, and their diameters were measured using National Institutes of Health (NIH) ImageJ software.

2.4. ATDC5 cell culture

An embryo derived, prechondrogenic cell line ATDC5 was used in this study. The cells were cultured in growth medium (GM) consisting of Dulbecco's Modified Eagle Medium/Nutrient Mixture F-12 Ham (DME/F-12, 1:1 mixture) supplemented with 1% 200 mM L-glutamine, 1% 10,000 U/mL penicillin/streptomycin, and 5% fetal bovine serum (FBS; Gibco, Waltham, MA, USA) during the preparation stage in flasks and before incubation in differentiation medium (DM). The DM used was GM supplemented with 1% 100 × insulin-transferrin-selenium (ITS) liquid media. The cells in the flasks were placed in serum-free GM for 24 h, suspended in GM, and seeded on the molecule- or fibril-coated coverslips in 24-well plates with 1.2×10^4 cells/well. The culture medium was replaced with DM 24 h after seeding, regarded as day 0. The medium was changed every 1–3 days. The cells from passages 4–9 were cultured at 100% humidity under 5% CO_2 at 37 °C.

2.5. ATDC5 morphology

A phase-contrast microscope (DMI600BM; Leica, Wetzlar, Germany) equipped with a time-lapse video system (STG/LASAF-FSH/1; Leica) was used to observe cell morphology responses to the molecule- and fibril-coated surfaces. Cell images were captured every 2.5 min for 6 h after cell seeding in the GM and 6 h after changing the GM to DM. SEM was also performed on days 0 (before the medium was changed to DM), 1, 3, 7, and 14. Coverslips with cells were treated as described in section 2.3, except for the fixation procedure; the medium was replaced with 10% (v/v) glutaraldehyde in PB (pH 7.6) and the samples were incubated for 10 min to prevent cell detachment.

2.6. ATDC5 growth and differentiation

ATDC5 growth was estimated using the CCK-8 assay kit (DOJINDO, Wako, Japan) on days 0 (before the medium was changed to DM), 1, 3, 7, and 14 following the user manual. Cell morphology was monitored using phase-contrast microscopy.

To monitor chondrocyte differentiation, AB staining was performed to confirm cartilage matrix production up to day 28. The cells were fixed in 95% methanol for 2 min, washed with HBSS, stained with 0.1% Alican blue (AB) 8GX (C.I. 74240; Sigma-Aldrich) in 0.1 M HCl solution, destained with distilled water, and imaged using a digital camera system (NOA630B; WRAYMER, Osaka, Japan) equipped with a light microscope (Eclipse E800; Nikon, Tokyo, Japan). All these procedures were conducted at 21 °C ± 5 °C, except for fixation at −30 °C.

2.7. Quantitative real-time polymerase chain reaction analysis

Total mRNA was extracted from the cells using ISOGEN II (Nippon gene, Toyama, Japan), and then treated with recombinant DNase I (TaKaRa, Kusatsu, Japan) and RNase Inhibitor (Nippon Gene) and refined using the phenol–chloroform method. Subsequently, the total RNA was reverse transcribed to cDNA using the PrimeScript RT Reagent Kit with gDNA Eraser (Perfect Real Time; TaKaRa). Quantitative real-time PCR (qPCR) was performed using the Fast Start Universal SYBR Green Master (Rox) (Roche, Mannheim, Germany) and LightCycler 96 (Roche). The relative mRNA expression of collagen type X alpha 1 (*Col10a1*), sex-determining region Y-box 9 (*Sox9*), aggrecan (*Acan*), and collagen type II alpha 1 (*Col2a1*) was determined using the $2^{-\Delta\Delta Ct}$ method [23] with peptidylprolyl lisomerase A (*Ppia*) as the internal reference. The specific primer sequences are shown in Table 1. The specificity of each positive reaction was confirmed using the melting temperature dissociation curves.

2.8. Statistical analysis

Numerical data are expressed as mean ± standard deviation. Two-sided Student's *t*-test was used to compare differences between the

Table 1
Primer sequences used for quantitative real-time PCR.

Primer	Forward sequence	Reverse sequence	Amplicon (bp)	Accession	Reference
Ppia	CGC GTC TCC TTC GAG CTG TTT G	TGT AAA GTC ACC ACC CTG GCA CAT	150	NM_008907.2	[24]
Sox9	CAA GAA CAA GCC ACA CGT CA	TGT AAT CGG GGT GGT CTT TC	221	NM_011448.4	[25]
Col10a1	CTG CTG CTA ATG TTC TTG AC	ACT GGA ATC CCT TTA CTC TTT	143	NM_009925.4	[25]
Acan	GCC TAC CCG GTA CCC TAC AG	ACA TTG CTC CTG GTC TGC AA	175	NM_007424.3	[25]
Col2a1	ATC TTG CCG CAT CTG TGT GT	CTC CTT TCT GCC CCT TTG GC	170	NM_031163.3	[25]

molecule- and fibril-coated groups during the same culture period. Microsoft Excel with add-in software (version 4.04; BellCurve, Tokyo, Japan) was used for statistical analyses.

3. Results

3.1. Fibril coating development

As the fibril-coating methods designed for type I collagen [26] cannot be applied to type II collagen owing to the high viscosity of type II collagen solution, the tailored "flip-contact method" was adapted. The amount of NC solution applied (20, 25, 30, and 35 μL/coverslip), coverslip surface type (non-coated PET-G coverslip [83.1840.002; Sarstedt K.K., Newton, NC, USA], non-coated glass coverslip [MATSUNAMI Glass Ind., LTD, Osaka, Japan], and ε-poly-L-lysine coated coverslip [MATSUNAMI Glass Ind.]), fibril formation time (48 and 72 h), and incubation temperature for fibril formation (4 °C, 12 °C, and 21 °C) were evaluated (Supplementary Figs. S1–S4). Finally, the optimum coating conditions were determined as described in Section 2.2. PET-G was chosen because of its good operational handle and the most stable and repeatable fibril morphology.

SEM observations revealed that the fibrils piled up in at least three layers (Fig. 1, a-b). A fine fibril layer at the bottom and a thick fibril layer covered the fine fibril layer. Amorphous material, which may be a molecule or semi-fibril-state collagen, was present in the middle layer (Fig. 1b). The fibril diameter was <50–500 nm; the mean diameter was 140.02 ± 74.62 nm (Fig. 1c).

3.2. Time-lapse analysis of ATDC5 cell behavior after seeding

ATDC5 cells attached to the molecule- and fibril-coated surfaces within 6 h of seeding (Fig. 2a, Videos 1 and 2). The cells gradually spread filopodia on both surfaces. Filopodia extension and retraction were more intense on the molecule-coated surface than on the fibril-coated surface (Videos 1 and 2). Furthermore, most cells on the fibril-coated surface were long and tapered. In contrast, those on the molecule-coated surface had diverse shapes—flat polygonal and tapered. In addition, the cells on the fibril-coated surface were smaller but thicker. Their positional movements were minimal, but their filopodia extended and retracted (Videos 1 and 2).

Supplementary video related to this article can be found at https://doi.org/10.1016/j.ocarto.2024.100450.

After 24 h, the GM was replaced with DM, and cell behavior was monitored for 6 h. The movement of the filopodia of the cells on both coatings became more dynamic than that in the GM, and cell migration was recorded. On the fibril-coated surface, most filopodia appeared as fine protrusions, and the cells repeatedly extended and retracted them. In contrast, on the molecule-coated surface, the filopodia varied in shape and rapidly changed the morphology. The cells on the molecule-coated surface migrated more actively than on the fibril-coated surface. The filopodia were constantly moving; however, the cell body on the fibrils was relatively small and the altitude was high; whereas, cells on the molecules were larger and flatter (Videos 3 and 4). Moreover, mitosis occurred in the molecule-coated group, but not in the fibril-coated group, within the monitored area, indicating that the cells on fibrils were proliferating slowly (Fig. 2b–Videos 3 and 4).

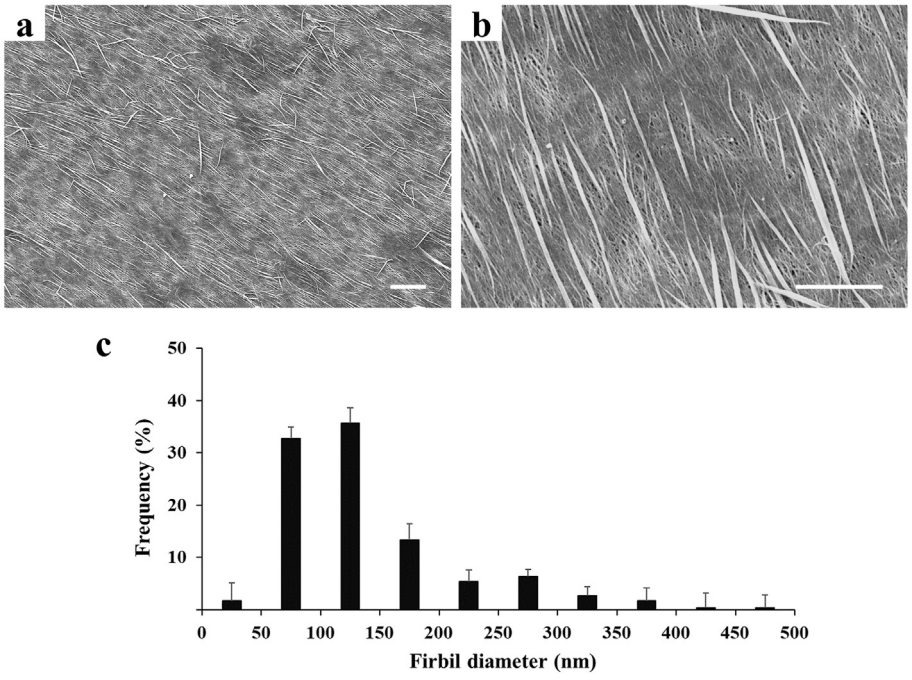

Fig. 1. Characteristics of the fibril-coated surface of the PET-G coverslip. Coating condition: 8 mg/mL notochord type II collagen solution, 30 mM phosphate buffer, 48 h fibril-formation time followed by 48 h crosslinking at 12 °C using the Flip-contact method. (a–b) Scanning electron microscopy images of the fibril-coated surface; scale bars, 10 μm (a) and 5 μm (b). (c) Fibril diameter distribution of the fibril-coated coverslip.

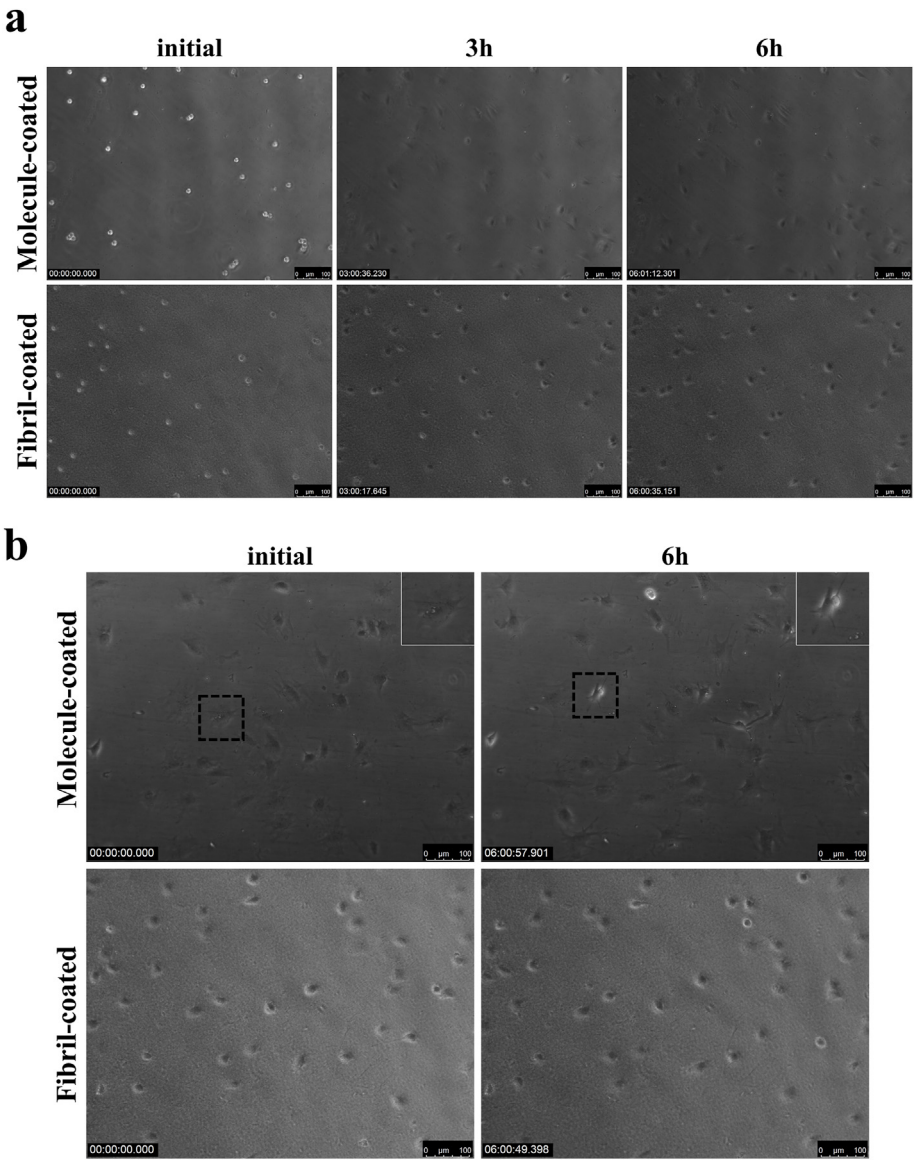

Fig. 2. Attachment and spreading of ATDC5 cells seeded on a type II collagen molecule-coated and fibril-coated coverslip. Photos were prepared from the freeze-frame of the time-lapse video for the initial time point and at 3 and 6 h. Scale bar, 100 μm. Cells were in growth medium (a) or differentiation medium (b).

Supplementary video related to this article can be found at https://doi.org/10.1016/j.ocarto.2024.100450.

In the fibril-coated group, long-tapered filopodia were consistently associated with cell bodies. The overall cell morphology remained similar during migration, with each cell showing a bulge in the middle and a flat area at its periphery. In the molecule-coated group, the cells actively moved the filopodia and changed their morphology. Therefore, the shape of each cell was more diverse in the molecule-coated group than in the fibril-coated group. Notably, the contact area between the cell body and the coating surface in the molecule-coated group rapidly increased, and the cells became more flattened when the medium was changed from GM to DM. In contrast, such cell morphology changes were not observed in the fibril-coated group during 30 h of monitoring (Fig. 2).

3.3. Scanning electron microscopy images of ATDC5 cells

In the molecule-coated group, the filopodia of cells increased in number with culture time until day 3 (Fig. 3a–c, f–h). Some filopodia extended until they reached other cells (Fig. 3f–h). The cell body gradually shrunk and was randomly shaped before the cells reached monolayer confluence (Fig. 3c). By day 7 (Fig. 3d and i), the cells grew upward on other cells, forming multiple layers. The cell morphology became indistinguishable, and the filopodia increased in number and length. On day 14 (Fig. 3e and j), the outline of each cell body was completely unrecognizable, and some filopodia of the top-layered cells laid over one another.

The cells on the fibril-coated surface had shorter filopodia than those on the molecule-coated surface on day 0 (Fig. 3k and p). Subsequently, the filopodia did not increase in number but extended (Fig. 3p–s). The cell body flattened and became round or oval when the cell number increased (Fig. 3k–o). On day 14 (Fig. 3o and t), the cells approached monolayer confluence and filopodia connected the cells.

3.4. Growth of ATDC5 cells

The CCK-8 assay revealed that ATDC5 cells grew rapidly on the molecule-coated surface. In contrast, they proliferated slowly on the fibril-coated surface on day 14 (Fig. 4). Slower proliferation on the fibril-coated surface was also confirmed in time-lapse monitoring experiments (Videos 1–2). The new cell cycle started within 6 h after seeding on the molecule-coated surface. However, cell proliferation was not observed on

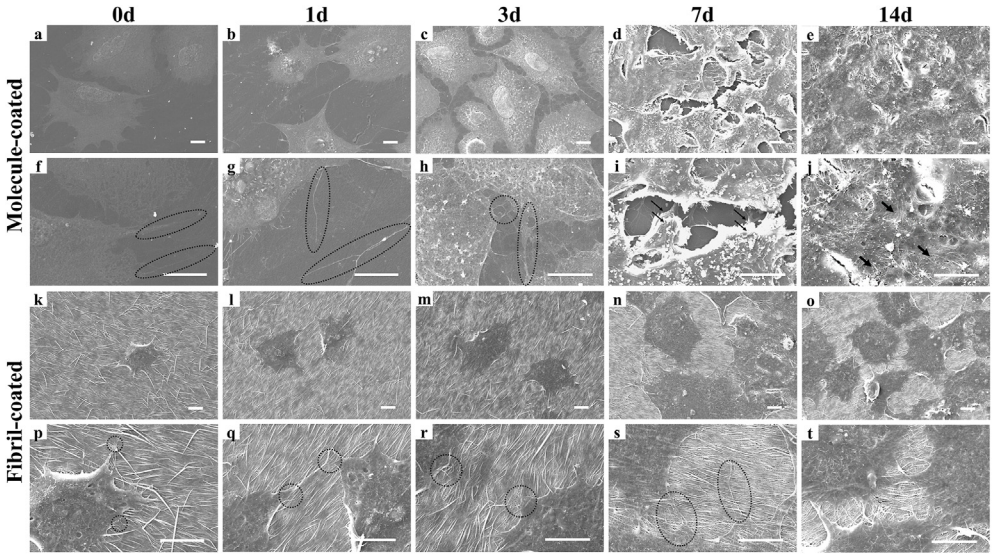

Fig. 3. Time-dependent changes of ATDC5 cell morphology under a scanning electron microscope on the molecule- and fibril-coated surfaces. After seeding cells and inducing attachment on the molecule- or fibril-coated coverslips for 24 h (day 0) in the growth medium, the medium was replaced with the differentiation medium, and the cells were further cultured for 14 days. Scale bar = 10 μm. f–j and p–t are the higher magnification images of a–e and k–o, respectively. Circles in f–h, extended filopodia; arrows in i, multi-layer of cells; arrows in j, cascading packed filopodia; circles in p–s, extended filopodia.

the fibril-coated surface. Cell proliferation quickly re-started on the molecule-coated surface when the medium was changed to DM. However, it started at the end of the 6 h-observation period on the fibril-coated surface. Phase-contrast microscopy revealed that the cells on the molecule-coated surface reached almost 100% confluency around day 3, but on the fibril-coated surface, the cells did not reach confluence even on day 14 (Fig. 5).

3.5. Alcian blue staining of extracellular secretions

AB staining is the conventional histological method to detect acidic polysaccharides (mainly chondroitin sulfate) secreted during chondrocyte differentiation. As presented in Fig. 6a, the molecule-coated surface without cells was negative for AB staining. When ATDC5 cells were cultured, the AB-positive area first appeared around the cells on day 14, suggesting that ECM secretion had started. However, no apparent deeper AB staining was observed until day 28. The fibril-coated surfaces stained faintly in the absence of cells. When ATDC5 cells were cultured, intense positive staining of AB started on day 14 (Fig. 6a), and intensely stained area increased when the culture period was extended to day 28. The staining area was also quantitatively measured (Supplementary Fig. S5).

In both groups, AB-staining appeared around the cell periphery, wherein the cells were closely packed and showed a round or oval morphology (Fig. 6b), representing the morphological phenotype of mature chondrocytes. In the fibril-coated group (Fig. 6b), gradual expansion of the deeply stained area after day 21 indicated that the differentiation stages of individual ATDC5 cells were not uniform under the same culture conditions. On day 28, the larger intense stained area in the fibril-coated group confirmed the continuous differentiation of cells and ECM-secretory activity reflected mature chondrocytes. In contrast, a deeply stained area did not appear in the molecule-coated group, despite the increased number of AB-positive cells. These findings suggest qualitative differences in AB-positive cells, resulting in a qualitative difference in the secreted materials between the groups.

3.6. Quantitative real-time PCR analysis

Gene expression levels were analyzed on days 14, 21, and 28 after transferring the cells into differentiation medium (Fig. 7). *Sox9* expression in the fibril-coated group was 5.21-times higher than that in the molecule-coated group (95% CI = 4.12–6.3, $p < 0.001$) only on day 21. On day 14, *Col10a1* expression in the fibril-coated group relative to that

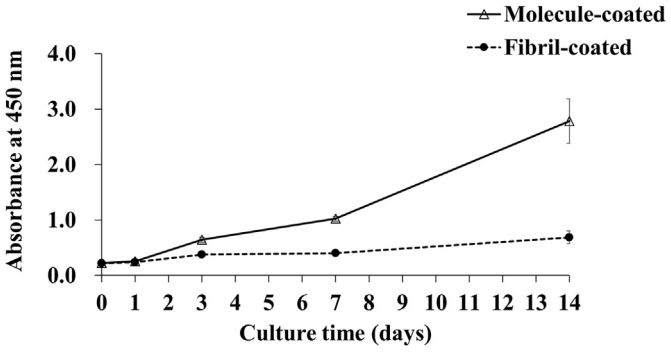

Fig. 4. Growth curves of ATDC5 cells cultured on the molecule- and fibril-coated surfaces. The cells were seeded and attachment was induced on the molecule- or fibril-coated surfaces for 24 h (day 0) in the growth medium; then, the medium was replaced with the differentiation medium, and the cells were further cultured for 14 days, $n = 3$–4.

in the molecule-coated group was 0.53 higher (95% CI = 0.38–0.67, $p = 0.0261$), showing a low expression at this time point; thereafter, the expression was 26.69-times (95% CI = 25.63–27.76, $p < 0.001$) and 24.15-times higher (CI = 0.14–48.16, $P = 0.0144$) on days 21 and 28, respectively. *Acan* expression in the fibril-coated group was higher than that in the molecule-coated group throughout the culture period: 2.51 times (95% CI = 0.85–4.17, $p = 0.0217$) on day 14, 19.49 times (95% CI = 15.6–23.38, $p < 0.001$) on day 21, and 7.02 times (95% CI = 1.57–12.47, $P = 0.0093$) on day 28. *Col2a1* expression on day 21 in the fibril-coated group was 5.5-times higher (95% CI = 2.33–8.67, $p = 0.0049$) than that in the molecule-coated group.

4. Discussion

In this study, the NC (type II collagen) was successfully self-assembled into a thin layer of fibrils *in vitro* using the "flip-contact method" and coated on a cell-culture coverslip, as the first NC fibril coating based on type II collagen from marine life. The diameter of most fibrils (50–150 nm) was close to that of fibrils in mature human cartilage [27]. Therefore, based on the morphology, the material developed in this study effectively mimicked human cartilage.

For CTE, the designed scaffold materials refer to the cartilage ECM, which is expected to facilitate efficient cell landing, chondrogenic differentiation, and chondrogenesis. Therefore, these materials must

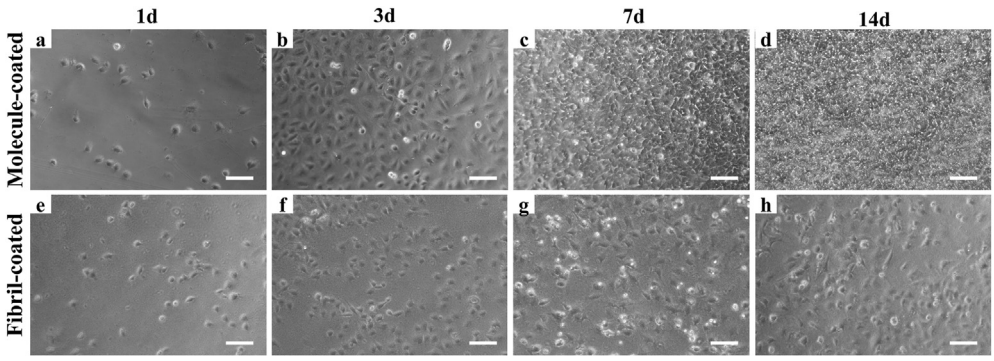

Fig. 5. Phase-contrast microscopy images of ATDC5 cells cultured on the molecule- and fibril-coated surfaces. After seeding the cells and inducing attachment on the coated coverslips for 24 h in the growth medium (day 0), the medium was replaced with the differentiation medium and maintained until day 14. Scale bar = 100 μm.

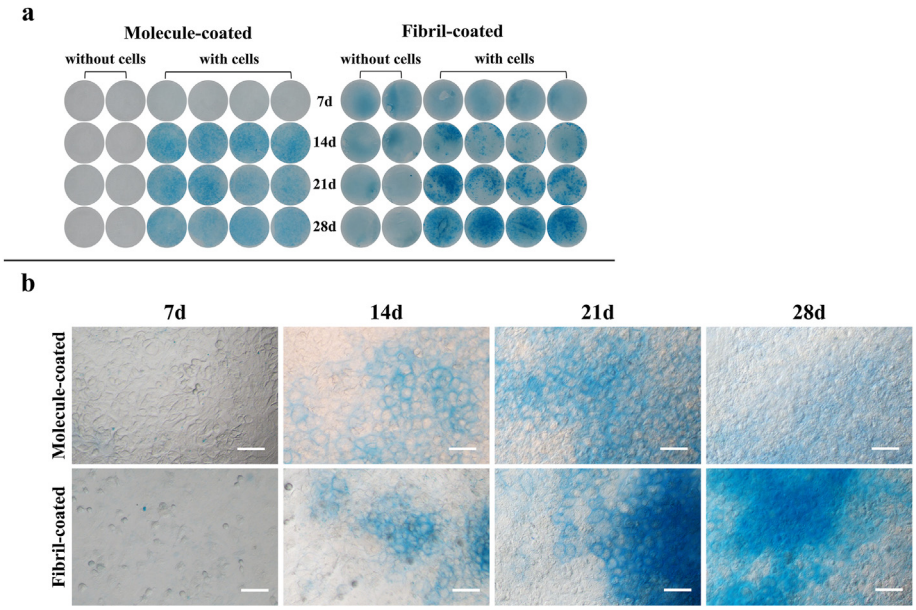

Fig. 6. Alcian blue (AB) staining of ATDC5 cells cultured on the molecule- and fibril-coated surfaces. a, photograph of the coverslips; b, photomicrograph of the AB-positive parts. Scale bar, 100 μm (b).

appropriately guide cellular signaling pathways for differentiation [11]. In this study, both the time-lapse observations and CCK-8 measurements consistently showed low proliferation and metabolic rates in the fibril-coated group (Figs. 2–5), directly highlighting the unique characteristics of type II fibrils (i.e., directly interfering with cell proliferation and altering metabolism). Combined with the ECM secretion by chondrocytes demonstrated subsequently in the fibril-coated group, we strongly suspect that the integrin-binding site offered by type II collagen fibrils affects the chondroinductive signaling pathway, altering the energy of the mitotic cycle for chondrogenesis. ECM production was higher and maintained persistently in the fibril-coated group, suggesting that the cells on the NC-fibrils maintained in the mature, functional chondrocyte stage. We also noted that on days 14 and 21, AB staining in the fibril group indirectly revealed the oval morphology of cells, thereby indicating the ability of fibrils to maintain the chondrocyte phenotype in the chondrogenic stage. These results illustrate that the type II fibril material, but not the molecular material, has chondroinductive ability. Notably, AB-staining was faintly positive on the fibril-coated surface without cells, probably because of chondroitin sulfate (CS) bound to type II collagen [28,29]. The NC is a hyaline cartilage-like tissue that contains CS, and complete separation of CS from type II collagen seems impossible under the employed purification conditions. Thus, the CS-laden state of the fibril material in this study may provide cells with a more appropriate microenvironment similar to *in vivo* conditions [6] to support chondroinduction because CS is beneficial for chondrogenesis [30].

Previous studies have reported the functionalities of bovine type I collagen hydrogels, bovine type II collagen sponges, and porcine type II hydrogels for cell-laden CTE research [8,12,30,32]. Marine collagens have also received attention as CTE materials [32–34] because of the lower risk of transferring zoonoses. For instance, porous materials made of type I collagen from blue shark skin and tilapia skin displayed chondroinductive ability [35,36]. Another study fabricated a porous material made of type II collagen from the jellyfish *Rhizostoma pulmo* [37]. However, the material displayed a weak ability to promote chondrogenesis. Porous materials made of four chondrichthyan cartilage type II collagens upregulated expression of the early chondrogenic marker *SOX9* and middle chondrogenic marker *ACAN*; nonetheless, *COL2A1* expression was not observed in any group [38]. In addition, type II materials are not made of collagen fibrils, which are natural collagens *in vivo*. Compared to these previously reported materials, NC fibril coating is advantageous because it uses type II collagen fibrils. In contrast, the cells grew two-dimensionally in this system; thus, three-dimensional cellular reactions could not be studied.

A thin layer of type II collagen fibrils enables conventional light microscopy, including time-lapse technology, to observe cellular movements. Therefore, this technology is effective for studying cellular reactions to type-

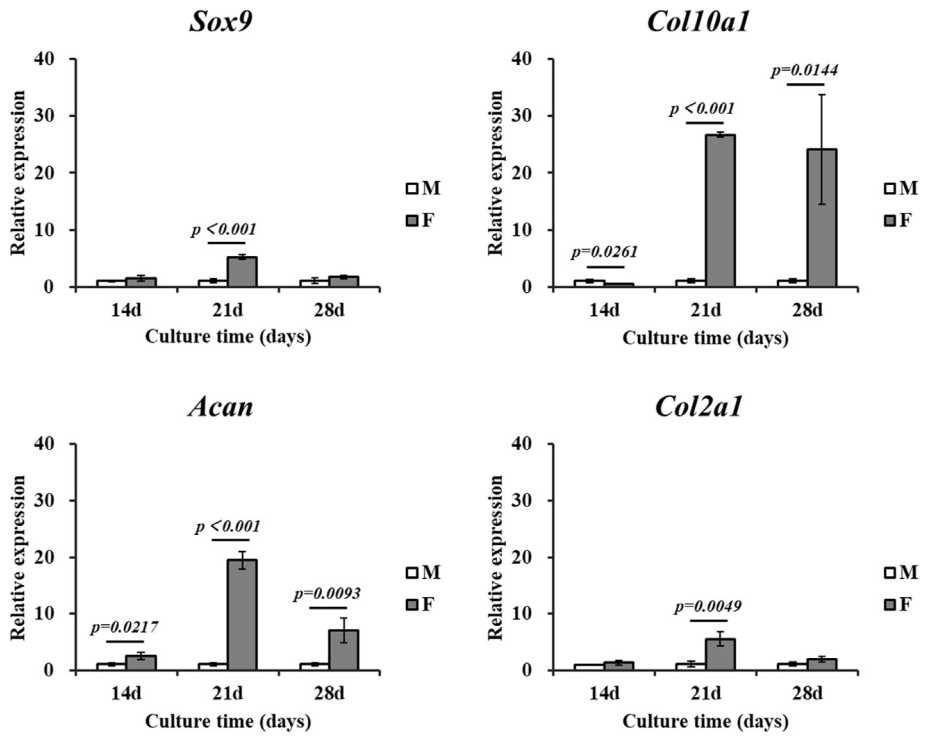

Fig. 7. mRNA expression levels in ATDC5 cells cultured on the fibril-coated surface (F) compared with those in ATDC5 cells cultured on the molecule-coated surface (M). Sex determining region Y-box 9 (a), collagen type X alpha 1 (b), aggrecan (c), and collagen type II alpha 1 (d), $n = 3$; the p-values indicate Student's t-test mean differences between the molecule- and fibril-coated groups.

II fibrils. Time-lapse monitoring revealed an inactive filopodium movement and cell migration on the fibril-coated surface. In addition, the filopodium morphology was almost a single protrusion, and the cell shape was more uniform on the fibrils. Moreover, the cells rapidly attached to the fibrils quickly stabilized their morphology and produced more cartilage ECMs than those on the molecules. We speculate that such differences in the ATDC5 responses to the fibrils and molecules arose from the specific binding sites of NC fibrils and specific integrin subunit expression of ATDC5. The transmembrane protein integrin, a heterodimeric complex of α and β subunits, contributes to filopodium formation and cellular adhesion to the pericellular matrix. Integrins are crucial to signal transduction between the ECM and cells, mediating gene expression by recognizing specific amino acid sequences, such as RGD and GFOGER, in ECM proteins [39]. The binding sites of type II collagen are primarily recognized by α10β1 and secondarily by α1β1 integrin [40]. Impaired integrin function generally affects cell adhesion, proliferation, differentiation, and survival by regulating the matrix-to-cell message delivery. This is also true for chondrocytes. For instance, an *ex vivo* culture of sectioned chicken sternal cartilage, in which β1-integrin function was blocked, showed increased apoptosis [41]. An *α1*-knockout mouse study revealed reduced mesenchymal cell proliferation and chondrogenesis-related mRNA expression [42].

The present study indicates that chondrogenic marker gene expression is upregulated when ATDC5 cells were cultured on the fibril-coated surface. Hence, we concluded that this type II collagen fibril material has a chondrogenesis-inducing ability and facilitates chondrogenic gene expression in cells. The simultaneous enhanced expression of *Sox9*, *Acan*, and *Col2a1*, which likely can be attributed to the induction of *Sox9* expression leading to the expression of *Acan* and *Col2a1* [43], indicated that chondrogenesis proceeded toward the middle stage in the present experiment. *Col10a1*, a marker gene of hypertrophic chondrocytes [44], also increased on day 21. We hypothesized that the increase in *Col10a1* mRNA expression during cell cultivation is insufficient to conclude that cells entered the hypertrophy stage in our study, especially under the condition of the simultaneous high expression of the early-stage chondrogenesis marker *Sox9* and the middle-stage markers *Acan* and *Col2a1*. *Col10a1* expression in ATDC5 cells in ascorbate-supplemented culture has been reported [45], and was upregulated with *Acan* and *Col2a1* in similar timing; Rubí-Sans et al. [46] also reported that strong *Col10a1* expression in human mesenchymal stem cells cultured on polycaprolactone materials when *Acan* and *Col2a1* upregulated. The results of a previous study by Wu et al. [38] support our hypothesis; using the chondrichthyan collagen scaffold cultured with human adipose-derived stem cells, they showed that the upregulated timing of *Col10a1* expressed was similar to *Sox9*. Moreover, a *Col10a1* knock-down research [47], shows the GAGs production required a small quantity of *Col10a1*. Hence, we adventure to the idea that *Col10a1* did not necessarily indicate the hypertrophic differentiation of cells and a high possibility related to the early chondrogenesis phase, and the proof of the existence and function of *Col10a1* in the early phase of chondrocyte differentiation remains to be solved in the future.

Therefore, we propose that the NC-fibril material activates partial signal pathways related to chondrogenesis in cells through integrin subunits. Through advantageous signal transduction, ATDC5 cells respond to the fibril material and functionalize as chondrocytes. Thus, the *in vitro* model presented herein may contribute to a better understanding of the molecular signaling pathways of chondrogenesis and might lead to further pharmacokinetic studies and/or CTE scaffold exploration in the future.

Author contributions

The conception and design of this study by LS and YT. The experiments were conducted by LS with the supervision and instructions of KU. All authors have been involved in the analysis and interpretation of the data and contributed to the final manuscript.

Role of the funding source

This work was supported by JST SPRING (Grant Number JPMJSP2119) to LS and a Grant-in-Aid for Challenging Research (Exploratory) 21K19130 from the Japan Society for the Promotion of Science to YT.

Data availability statement

All data that support the findings of this study are included within the article (and any supplementary files).

Declaration of competing interest

The authors declare that they have no known competing financial interests or personal relationships that could have influenced the work reported in this paper.

Acknowledgments

We would like to thank Editage (www.editage.com) for English language editing.

Appendix A. Supplementary data

Supplementary data to this article can be found online at https://doi.org/10.1016/j.ocarto.2024.100450.

References

[1] J. Riesle, A.P. Hollander, R. Langer, L.E. Freed, G. Vunjak-Novakovic, Collagen in tissue-engineered cartilage: types, structure, and crosslinks, J. Cell Biol. 71 (1998) 313–327, https://doi.org/10.1002/(sici)1097-4644(19981201)71:3<313::aid-jcb1>3.0.co;2-c.
[2] D.R. Eyre, Collagens and cartilage matrix homeostasis, Clin. Orthop. Relat. Res. 427 (2004) S118–S122, https://doi.org/10.1097/01.blo.0000144855.48640.b9.
[3] T. Hardingham, M. Bayliss, Proteoglycans of articular cartilage: changes in aging and in joint disease, Semin. Arthritis Rheum. 20 (1990) 12–33, https://doi.org/10.1016/0049-0172(90)90044-G.
[4] D.J. Huey, J.C. Hu, K.A. Athanasiou, Unlike bone, cartilage regeneration remains elusive, Science 338 (2012) 917–921, https://doi.org/10.1126/science.1226418.
[5] H.A. Wieland, M. Michaelis, B.J. Kirschbaum, K.A. Rudolphi, Osteoarthritis - an untreatable disease? Nat. Rev. Drug Discov. 4 (2005) 331–344, https://doi.org/10.1038/nrd1693.
[6] D.R. Eyre, M.A. Weis, J.J. Wu, Articular cartilage collagen: an irreplaceable framework? Eur. Cell. Mater. 12 (2006) 57–63, https://doi.org/10.22203/eCM.v012a07.
[7] F. Davatchi, B.A. Abdollahi, M. Mohyeddin, F. Shahram, B. Nikbin, Mesenchymal stem cell therapy for knee osteoarthritis. Preliminary report of four patients, Int. J. Rheum. Dis. 14 (2011) 211–215, https://doi.org/10.1111/j.1756-185X.2011.01599.x.
[8] L. Zhang, T. Yuan, L. Guo, X. Zhang, An in vitro study of collagen hydrogel to induce the chondrogenic differentiation of mesenchymal stem cells, J. Biomed. Mater. Res. A. 100 (2012) 2717–2725, https://doi.org/10.1002/jbm.a.34194.
[9] K.M. Pawelec, S.M. Best, R.E. Cameron, Collagen: a network for regenerative medicine, J. Mater. Chem. B 4 (2016) 6484–6496, https://doi.org/10.1039/c6tb00807k.
[10] K.D. Ngadimin, A. Stokes, P. Gentile, A.M. Ferreira, Biomimetic hydrogels designed for cartilage tissue engineering, Biomater. Sci. 9 (2021) 4246–4259, https://doi.org/10.1039/d0bm01852j.
[11] V. Irawan, T.C. Sung, A. Higuchi, T. Ikoma, Collagen scaffolds in cartilage tissue engineering and relevant approaches for future development, Tissue Eng. Regen. Med. 15 (2018) 673–697, https://doi.org/10.1007/s13770-018-0135-9.
[12] J. Yang, Y. Xiao, Z. Tang, L. Zhaocong, D. Li, Q. Wang, et al., The negatively charged microenvironment of collagen hydrogels regulates the chondrogenic differentiation of bone marrow mesenchymal stem cells in vitro and in vivo, J. Mater. Chem. B 8 (2020) 4680–4693, https://doi.org/10.1039/d0tb00172d.
[13] B.B. Christensen, C.B. Foldager, J. Jensen, N.C. Jensen, M. Lind, Poor osteochondral repair by a biomimetic collagen scaffold: 1- to 3-year clinical and radiological follow-up, Knee Surg. Sports Traumatol. Arthrosc. 24 (2016) 2380–2387, https://doi.org/10.1007/s00167-015-3538-3.
[14] P. Buma, J.S. Pieper, T. van Tienen T, J.L.C. van Susante, P.M. van der Kraan, J.H. Veerkamp, et al., Cross-linked type I and type II collagenous matrices for the repair of full-thickness articular cartilage defects - a study in rabbits, Biomaterials 24 (2003) 3255–3263, https://doi.org/10.1016/S0142-9612(03)00143-1.
[15] Z. Wu, S. Korntner, A. Mullen, D. Zeugolis, Collagen type II: from biosynthesis to advanced biomaterials for cartilage engineering, Biomater. Biosyst. 4 (2021) 100030, https://doi.org/10.1016/j.bbiosy.2021.100030.
[16] L. Merly, S.L. Smith, Collagen type II, alpha 1 protein: a bioactive component of shark cartilage, Int. Immunopharm. 15 (2013) 309–315, https://doi.org/10.1016/j.intimp.2012.12.001.
[17] M. Maepa, M. Razwinani, S. Motaung, Effects of resveratrol on collagen type II protein in the superficial and middle zone chondrocytes of porcine articular cartilage, J. Ethnopharmacol. 178 (2016) 25–33, https://doi.org/10.1016/j.jep.2015.11.047.
[18] C. Ma, M. Yu, Z. Huang, J. Wang, X. Zhao, C. Kang, et al., Oral administration of hydrolysates of cartilage extract in the prevention of osteoarthritis, J. Funct.Foods 78 (2021) 104376, https://doi.org/10.1016/j.jff.2021.104376.
[19] I. Laasri, M. Bakkali, L.M. Torrent, A. Laglaoui, Marine collagen: unveiling the blue resource-extraction techniques and multifaceted applications, Int. J. Biol. Macromol. 253 (2023) 127253, https://doi.org/10.1016/j.ijbiomac.2023.127253.
[20] P. Kittiphattanabawon, S. Benjakul, W. Visessanguan, F. Shahidi, Isolation and characterization of collagen from the cartilages of brownbanded bamboo shark (Chiloscyllium punctatum) and blacktip shark (Carcharhinus limbatus), LWT 43 (2010) 792–800, https://doi.org/10.1016/j.lwt.2010.01.006.
[21] D. Meng, H. Tanaka, T. Kobayashi, H. Hatayama, X. Zhang, K. Ura, et al., The effect of alkaline pretreatment on the biochemical characteristics and fibril-forming abilities of types I and II collagen extracted from bester sturgeon by-products, Int. J. Biol. Macromol. 131 (2019) 572–580, https://doi.org/10.1016/j.ijbiomac.2019.03.091.
[22] P. Bronzi, M. Chebanov, J.T. Michaels, Q. Wei, H. Rosenthal, J. Gessner, Sturgeon meat and caviar production: global update 2017, J. Appl. Ichthyol. 35 (2019) 257–266, https://doi.org/10.1111/jai.13870.
[23] T.D. Schmittgen, K.J. Livak, Analyzing real-time PCR data by the comparative CT method, Nat. Protoc. 3 (2008) 1101–1108, https://doi.org/10.1038/nprot.2008.73.
[24] Z. Zhai, Y. Yao, Y. Wang, Importance of suitable reference gene selection for quantitative RT-PCR during ATDC5 cells chondrocyte differentiation, PLoS One 8 (2013) 5, https://doi.org/10.1371/journal.pone.0064786.
[25] J.K. Hodax, J.B. Quintos, P.A. Gruppuso, Q. Chen, S. Desai, C.T. Jayasuriya, Aggrecan is required for chondrocyte differentiation in ATDC5 chondroprogenitor cells, PLoS One 14 (2019) 6, https://doi.org/10.1371/journal.pone.0218399.
[26] S. Moroi, T. Miura, T. Tamura, X. Zhang, K. Ura, Y. Takagi, Self-assembled collagen fibrils from the swim bladder of Bester sturgeon enable alignment of MC3T3-E1 cells and enhance osteogenic differentiation, Mater. Sci. Eng., C 104 (2019) 109925, https://doi.org/10.1016/j.msec.2019.109925.
[27] A.N. Buxton, J. Zhu, R. Marchant, J.L. West, J.U. Yoo, B. Johnstone, Design and characterization of poly(ethylene glycol) photopolymerizable semi-interpenetrating networks for chondrogenesis of human mesenchymal stem cells, Tissue Eng. 13 (2007) 2549–2560, https://doi.org/10.1089/ten.2007.0075.
[28] E.J. Miller, M.B. Mathews, Characterization of notochord collagen as a cartilage-type collagen, Biochem. Biophys. Res. Commun. 60 (1974) 424–430, https://doi.org/10.1016/0006-291x(74)90221-6.
[29] S. Jahn, J. Seror, J. Klein, Lubrication of articular cartilage, Annu. Rev. Biomed. Eng. 18 (2016) 235–258, https://doi.org/10.1146/annurev-bioeng-081514-123305.
[30] X. Ren, F. Wang, C. Chen, X. Gong, L. Yin, L. Yang, Engineering zonal cartilage through bioprinting collagen type II hydrogel constructs with biomimetic chondrocyte density gradient, BMC Muscoskel. Disord. 17 (2016) 301, https://doi.org/10.1186/s12891-016-1130-8.
[31] C.S. Ko, J.P. Huang, C.W. Huang, I.M. Chu, Type II collagen-chondroitin sulfate-hyaluronan scaffold cross-linked by genipin for cartilage tissue engineering, J. Biosci. Bioeng. 107 (2009) 177–182, https://doi.org/10.1016/j.jbiosc.2008.09.020.
[32] B. Hoyer, A. Bernhardt, A. Lode, S. Heinemann, J. Sewing, M. Klinger, et al., Jellyfish collagen scaffolds for cartilage tissue engineering, Acta Biomater. 10 (2014) 883–892, https://doi.org/10.1016/j.actbio.2013.10.022.
[33] M. Khajavi, A. Hajimoradloo, M. Zandi, M. Pezeshki-Modaress, S. Bonakdar, A. Zamani, Fish cartilage: a promising source of biomaterial for biological scaffold fabrication in cartilage tissue engineering, J. Biomed. Mater. Res. A. 109 (2021) 1737–1750, https://doi.org/10.1002/jbm.a.37169.
[34] W. Li, K. Ura, Y. Takagi, Industrial application of fish cartilaginous tissues, Curr. Res. Food Sci. 5 (2022) 698–709, https://doi.org/10.1016/j.crfs.2022.04.001.
[35] G.S. Diogo, F. Carneiro, S. Freitas-Ribeiro, C.G. Sotelo, R.I. Pérez-Martín, R.P. Pirraco, et al., Prionace glauca skin collagen bioengineered constructs as a promising approach to trigger cartilage regeneration, Mater. Sci. Eng., C 120 (2021) 111587, https://doi.org/10.1016/j.msec.2020.111587.
[36] H. Li, R. Chen, Z. Jia, C. Wang, Y. Xu, C. Li, et al., Porous fish collagen for cartilage tissue engineering 12 (2020) 6107–6121.
[37] M. Pugliano, X. Vanbellinghen, P. Schwinté, N. Benkirane-Jessel, L. Keller, Combined jellyfish collagen type II, human stem cells and Tgf-β3 as a therapeutic implant for cartilage repair, J. Stem Cell Res. Ther. 7 (2017) 4, https://doi.org/10.4172/2157-7633.1000382.
[38] Z. Wu, S.H. Korntner, A.M. Mullen, D.I. Zeugolis, In the quest of the optimal chondrichthyan for the development of collagen sponges for articular cartilage, J. Sci.-Adv. Mater. Dev. 6 (2021) 390–398, https://doi.org/10.1016/j.jsamd.2021.04.002.
[39] C.G. Knight, L.F. Morton, A.R. Peachey, D.S. Tuckwell, R.W. Farndale, M.J. Barnes, The collagen-binding A-domains of Integrins α1β1 and α2β1 recognize the same specific amino acid sequence, GFOGER, in native (triple-helical) collagens, J. Biol. Chem. 275 (2000) 35–40, https://doi.org/10.1074/jbc.275.1.35.
[40] R.F. Loeser, Chondrocyte integrin expression and function, Biorheology 37 (2000) 109–116.
[41] M.S. Hirsch, E. Lunsford, V. Trinkaus-Randall, K.K.H. Svoboda, Chondrocyte survival and differentiation in situ are integrin mediated, Dev. Dynam. 210 (1997) 249–263, https://doi.org/10.1002/(SICI)1097-0177(199711)210:3<249::AID-AJA6>3.0.CO;2-G.
[42] E. Ekholm, K.D. Hankenson, H. Uusitalo, A. Hiltunun, H. Gardner, J. Heino, et al., Diminished callus size and cartilage synthesis in α1β1 integrin-deficient mice during bone fracture healing, Am. J. Pathol. 160 (2002) 1779–1785, https://doi.org/10.1016/S0002-9440(10)61124-8.

[43] D.M. Bell, K.K.H. Leung, S.C. Wheatley, L.J. Ng, S. Zhou, K.W. Ling, et al., SOX9 directly regulates the type-II collagen gene, Nat. Genet. 16 (1997) 174–178, https://doi.org/10.1038/ng0697-174.
[44] Y. Luo, D. Sinkeviciute, Y. He, M. Karsdal, Y. Henrotin, A. Mobasheri, et al., The minor collagens in articular cartilage, Protein Cell 8 (2017) 560–572, https://doi.org/10.1007/s13238-017-0377-7.
[45] F.M. Altaf, T.M. Hering, N.H. Kazmi, J.U. Yoo, B. Johnstone, Ascorbate-enhanced chondrogenesis of ATDC5 cells, Eur. Cell. Mater. 12 (2006) 64–69, https://doi.org/10.22203/ecm.v012a08.
[46] G. Rubí-Sans, L. Recha-Sancho, S. Pérez-Amodio, M.Á. Mateos-Timoneda, C.E. Semino, E. Engel, Development of a three-dimensional bioengineered platform for articular cartilage regeneration, Biomolecules 10 (2020) 52, https://doi.org/10.3390/biom10010052.
[47] C.A. Knuth, E.A. Sastre, N.B. Fahy, J. Witte-Bouma, Y. Ridwan, E.M. Strabbing, et al., Collagen type X is essential for successful mesenchymal stem cell-mediated cartilage formation and subsequent endochondral ossification, Eur. Cell. Mater. 38 (2019) 106–222, https://doi.org/10.22203/eCM.v038a09.